

INSTITUT DE FRANCE  
Académie des sciences

# *Comptes Rendus*

---

## *Chimie*

Poulomi Chandra, Diptiman Choudhury and Anoop Verma

**Electrooxidation treatment of simulated wastewater using mixed-metal oxide anodes for bacterial decontamination**


Volume 26, Special Issue S1 (2023), p. 129-144

Online since: 23 March 2023

**Part of Special Issue:** Materials and Clean Processes for Sustainable Energy and Environmental Applications

**Guest editors:** Mejdi Jeguirim (Université de Haute-Alsace, Institut de Sciences des Matériaux de Mulhouse, France) and Patrick Dutournié (Université de Haute-Alsace, Institut de Sciences des Matériaux de Mulhouse, France)

<https://doi.org/10.5802/crchim.225>

 This article is licensed under the  
CREATIVE COMMONS ATTRIBUTION 4.0 INTERNATIONAL LICENSE.  
<http://creativecommons.org/licenses/by/4.0/>



*The Comptes Rendus. Chimie are a member of the  
Mersenne Center for open scientific publishing*  
[www.centre-mersenne.org](http://www.centre-mersenne.org) — e-ISSN : 1878-1543

## Materials and Clean Processes for Sustainable Energy and Environmental Applications

# Electrooxidation treatment of simulated wastewater using mixed-metal oxide anodes for bacterial decontamination

Poulomi Chandra <sup>a</sup>, Diptiman Choudhury <sup>\*,a,b</sup> and Anoop Verma <sup>\*,\*,b,c</sup>

<sup>a</sup> School of Chemistry and Biochemistry, Thapar Institute of Engineering and Technology (TIET), Patiala, Punjab-147004, India

<sup>b</sup> TIET-VT (Virginia Tech-USA) Centre of Excellence for Emerging Materials (CEEMS), Thapar Institute of Engineering and Technology, Patiala, Punjab-147004, India

<sup>c</sup> School of Energy and Environment, Thapar Institute of Engineering and Technology (TIET), Patiala, Punjab-147004, India

E-mails: pchandra\_phd19@thapar.edu (P. Chandra), diptiman@thapar.edu (D. Choudhury), anoop.kumar@thapar.edu (A. Verma)

**Abstract.** This study aims to explore the potential use of electro-oxidation (EO) as a decentralized wastewater treatment method. The simulated wastewater comprising bacterial consortium was treated by employing mixed metal oxide (MMO). In particular, a lab-scale batch electrooxidation reactor was used at different operating parameters including NaCl dose ( $n$ ), current density ( $j$ ), and treatment time ( $t$ ) in order to optimize the process using response surface methodology. The efficiency of the treatment process was evaluated in terms of % inactivation and energy consumption which were found to be 99.2% and 0.42 kWh/m<sup>3</sup>, respectively. Under optimal conditions, it was found that the proposed technique's overall operating cost was 0.189 \$/m<sup>3</sup> taking into consideration the electrical energy consumed and cost of electrodes.

**Keywords.** Electrooxidation, Response surface methodology, Bacterial consortium, Decentralized treatment, Water-based pandemic.

*Manuscript received 4 November 2022, revised 22 December 2022 and 27 January 2023, accepted 6 February 2023.*

## 1. Introduction

The presence of microbial populations in nearby water bodies like ground and surface water and their downstream effects is always a point of concern for developing nations. The main reason includes

the contamination through the untreated or partially treated wastewaters from different sources. This contamination affects the water cycle through chain reaction, thereby contaminating the whole ecosystem and affecting the human health [1]. The established conventional treatment technologies like membrane [2], adsorption [3] and ozonation [4] techniques, along with advanced oxidation processes like photocatalysis [5], Fenton based oxidation pro-

\*Corresponding author

cess [6], are effective in removing organic and inorganic contaminants from wastewater. However, their efficiency towards handling the microbial load and the volume of wastewater in large treatment plants remains a big concern [7]. There may be different sources of the microbial population like the food industry, laboratories, and domestic households. But, the wastewater coming from health care facilities poses a big challenge for the conventional treatment system for their effective removal. More specifically, discharge from infected wards of hospitals poses a serious threat to public health due to the presence of microbes of different pathogenicity levels [8]. With the emergence of new viral strains like COVID-19 and the spread of infection, there is an urgent need for a decentralized treatment system using novel technologies to avoid future water-based pandemics.

In this context, the present study reports the requirement of a cost-effective decentralized wastewater treatment system in terms of electrooxidation (EO) for tackling the pathogens/microbial load as per their origin before heading to the sewage treatment plant (STP).

As discussed, an on-site treatment facility for the ward-specific wastewater is needed for the hour before it mixes with the common effluent. In recent years, the conventional methods have been replaced by advanced technologies, which are more reliable for eliminating many pathogenic microorganisms from wastewater [9–12]. These technologies have made extensive advancements in treating wastewater due to their high efficiency and high oxidation stability [13]. One of the most affordable and interesting techniques for the ward-specific treatment of wastewater is electrooxidation (EO) [14–18]. EO is a versatile, eco-friendly, and cost-effective technique. The EO commercial-scale feasibility depends on the electrode material capable of generating various chloro-oxidant species and hydroxyl radicals [19].

The efficacy of the EO process mainly depends on the type of electrodes. Several authors have reported the removal of microbes from human urine by using boron-doped diamond (BDD) [20]. Despite excellent compatibility, performance, and high oxidation potential [21,22], BDD is unsuitable for commercial-scale application because of its high cost and toxic by-products formation [21].

The application of mixed metal oxide (MMO) electrode has been extensively studied in the literature.

This great interest is mainly due to its low production cost and the high electrochemical stability that promotes the formation of reactive chlorine species (RCS) and reactive oxygen species (ROS) at a low current density which is essential as compared to BDD [22–26]. The MMO anodes have shown a variety of applications for the treatment of synthetic wastewater [27], paper mill water [28], pesticides, pharmaceuticals, dyes, phenols, and real wastewater [23,24,29,30].

In this experimental study, the novel quaternary MMO anodes Ti/Ir/Ru/Pt have been selected for the EO treatment of simulated wastewater containing bacteria. In order to get more active sites, stability at high temperature and acidic solutions, durability, resistivity, and electrochemical stability at low current densities, this novel combination of metal oxides were incorporated into the titanium anodes [31]. This study further claims the first-time use of this ternary MMO anodes for the EO treatment of bacteria.

The inactivation of bacteria through EO treatment generally occurs by damaging the bacterial cells. Firstly, the produced RCS damages the cell membrane permeability, leading to enzymatic changes in the bacterial cell. Secondly, the damage to the cell membrane leads to the impairment of intracellular components, thereby causing the loss of deoxyribonucleic acid integrity [32].

Although studies on the disinfection of bacteria in different wastewater by EO have been reported [9,33–35], yet there are hardly any commercial success stories. Major reason could be its approach as an end-of-pipe treatment where handling of large volume of wastewater makes the process unfeasible on a commercial scale. Through this study EO is proposed to be a reactive approach where it can a ward-specific technique handling small volumes of waste water, thus can be a viable solution. Moreover, efficiency of any advanced technology is always more when it is applied to low volumes. In order to validate the proposed model, a simulated wastewater with bacterial consortium was taken for EO treatment for checking its efficacy for the inactivation of bacteria with minimum range of current density and electrolyte dose, which further validates the concept for this technology to be a decentralized treatment system.

Within this background, the main objective of the present work is to analyze the complete disinfection

of simulated wastewater of bacterial consortium employing electrolysis using MMO anodes, paying special attention to the durability of anodes. Anode's durability and stability were analyzed through characterization techniques like SEM-EDS, XPS, XRD, cyclic voltammetry. The influence of various parameters like current density, electrolyte concentration (NaCl), and treatment time on bacterial inactivation was studied through response surface methodology (RSM). This study aimed to evaluate the efficiency of the EO technique alone for removing bacteria from simulated wastewater using MMO anodes through batch mode in a laboratory-scale reactor.

## 2. Material and methods

### 2.1. Chemicals and microorganisms

Sodium sulphate with 99% purity, potassium acetate ( $\text{CH}_3\text{CO}_2\text{K}$ ), sodium hydroxide (NaOH), sulfuric acid ( $\text{H}_2\text{SO}_4$ ), sodium chloride (NaCl) of analytical grade, and terephthalic acid with 99% purity were purchased from Loba Chemicals Pvt. Ltd., India. Terephthalic acid was used to estimate the hydroxyl radical formation in the EO process. Luria Bertani broth was purchased from HiMedia Laboratories Pvt. Ltd. Mumbai, India. All the bacterial strains in the present study, *Escherichia coli* (MTCC no. 448), *Bacillus subtilis* (MTCC no. 441), *Staphylococcus aureus* (MTCC no. 902), *Salmonella enterica* (MTCC no. 1165), *Acinetobacter calcoaceticus* (MTCC no. 1948), *Serratia marcescens* (MTCC no. 2645), *Listeria sp.* (MTCC no. 4214), *Enterococcus faecalis* (MTCC no. 6845) were obtained from IMTech, Chandigarh, India. In this study, these eight different bacterial strains were chosen since they commonly found in hospital wastewater [36]. These bacteria were analyzed separately by varying the current density and electrolyte concentration range as reported previously [8]. All the solutions were prepared in double-distilled water of high purity.

### 2.2. Sample preparation and experimental setup

EO treatment of the simulated wastewater was carried out in a batch reactor. The simulated wastewater was prepared by dissolving 3.5 g of potassium acetate, 400 mg of sodium sulfate, and 5 mL of glacial

acetic acid in 1 L of double-distilled water. This simulated wastewater containing inorganic salts simulates the composition of human urine. The concentration of sodium chloride was varied according to the reaction. The bacterial culture from log phase was taken. This culture was grown up to an absorbance range of 0.8–1.0 nm by inoculating 1–2  $\mu\text{L}$  of bacterial strain in Luria Broth. The concentration of bacterial culture in the test solution was calculated in accordance with the absorbance of the bacterial culture. The simulated wastewater solution was freshly prepared each time. The EO treatment of simulated wastewater was carried out in a batch mode in a glass reactor having a working volume of 300 mL, as shown in Figure 1. The MMO anode used in this study was purchased from Tiaano Pvt. Ltd., Chennai, India. The MMO anode was composed of a titanium sheet coated with iridium, ruthenium, and platinum oxides. The stainless-steel cathode was purchased from a local vendor in Mohali, India. The dimension of the electrodes was (70 mm  $\times$  70 mm  $\times$  1 mm) with a surface area of 42  $\text{cm}^2$  (10 mm inter-electrode spacing). The DC power supply was purchased from (GAYATRI ENGINEERS, Maharashtra, India, Model: 0–30 V, 0–2 A) to maintain the current density for each experimental run. The magnetic stirrer was used at 500–550 RPM to maintain the homogeneity of the electrolyte concentration in the sample. All the experiments were performed three times to ensure the reproducibility of results. All the samples were collected at a specific time interval of 1 min.

### 2.3. Analytical methods

The analytical studies of bacterial inactivation were carried out by analyzing the bacterial samples through a UV-visible spectrophotometer at 600 nm. The inactivation of bacteria was also confirmed by plating the initial and final samples on Luria agar plates and incubating them in an incubator for 24 h. The hydroxyl radical ( $\text{OH}\cdot$ ) study was done using a fluorescence spectrophotometer (Shimadzu RF 6000) during the EO process. The terephthalic acid (TPA) used reacts with  $\text{OH}\cdot$  in the EO process [37] and produces a fluorescent compound 2-hydroxy terephthalic acid (TAOH). The intensity of this fluorescent compound was taken at an excitation wavelength of 315 nm and an emission wavelength of 425 nm. Total available chlorine (TAC) analysis

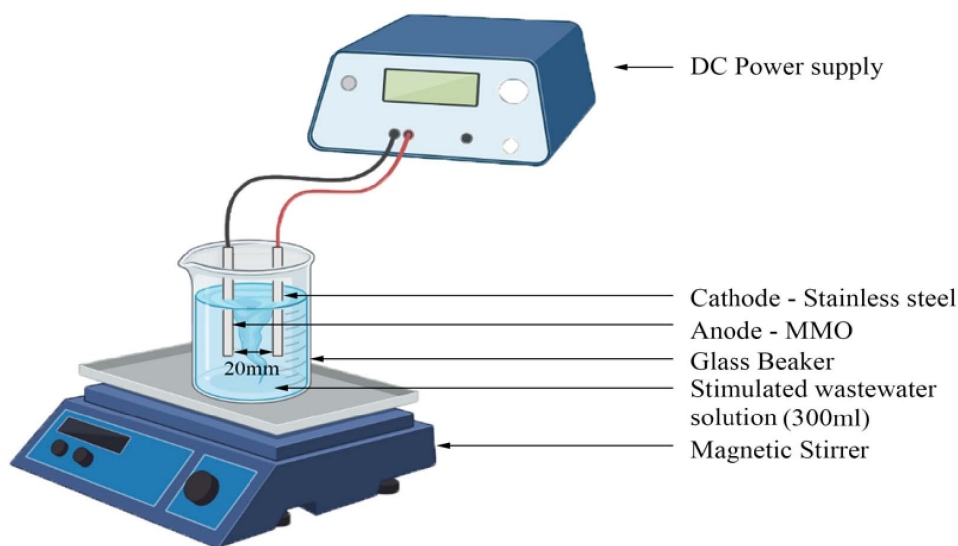


**Figure 1.** Schematic representation of electrooxidation setup under batch mode with mixed metal oxide anode and stainless-steel cathode.

was done to check the amount of chlorine produced during the EO process. TAC analysis was performed for the untreated and treated simulated wastewater samples by APHA standard (4500-Cl B) method. The surface morphology and elemental composition of MMO anodes were executed by SEM-EDS (JSM-6510LV, JEOL, Japan).

The electronic state of the MMO anodes was analyzed by XPS (X-ray photoelectron spectroscopy (PHI 5000 Versa-Probe III, Physical Electronics)). The potassium ion leakage test was performed by APHA: 3500 K method, which confirmed the inactivation of bacteria in untreated and treated simulated wastewater samples.

#### 2.4. Experimental procedure

The EO treatment of the simulated wastewater containing eight different bacteria was carried out under galvanostatic conditions. The pH of the working sample was adjusted accordingly by 1N HCl and 1N NaOH. The experimental reaction was carried out at an original pH of 4.25. The conductivity of the simulated wastewater solution was improved by adding NaCl as a supporting electrolyte. The initial conductivity of the sample solution was around 2.5 mS. The NaCl concentration and current density were varied according to the experimental reaction. At specific

time intervals, 100  $\mu$ L of the sample solution was taken and was inoculated in 5 mL of Luria broth. The samples were then incubated for 24 h in an incubator. After 24 h, the samples were analyzed spectrophotometrically at a wavelength of 600 nm to measure the absorbance of the samples for determination of % inactivation of bacteria. After each experimental run, the electrodes were washed by dipping them in a 5%  $\text{H}_2\text{SO}_4$  solution. The complete inactivation of the bacteria was observed within a short period of time. Thus, the efficacy of the EO process was proved in terms of the inactivation of bacteria.

#### 2.5. Experimental design and analysis

Response Surface Methodology (RSM), a three-level Box-Behnken design (BBD) based statistical technique is used to optimize the operational parameters as well as to reduce the number of experimental runs. In addition, it is used to analyze inter-parametric interactions of the input parameters and their effects on the responses [38]. The RSM technique works according to the equation  $N = s^2 + s + m_p$ , where  $s$  is the number of factors and  $m_p$  is the replicating number of central points [39]. The three initial input parameters in this study are NaCl dose ( $n$ ) ( $X_1$ ), current density ( $j$ ) ( $X_2$ ), and treatment time ( $t$ ) ( $X_3$ ) which were

**Table 1.** The experimental results of BBD matrix for electrooxidation treatment of simulated wastewater

Std	Run	Block	NaCl dose (g/L)	Current density (mA/cm <sup>2</sup> )	Time (min)	% Inactivation	Energy consumption (kWh/m <sup>3</sup> )
6	1	Block 1	2.50	7.14	2.00	17.79	0.1254
12	2	Block 1	1.50	11.90	16.00	99.61	1.995
15	3	Block 1	1.50	7.14	9.00	96.71	0.525
16	4	Block 1	1.50	7.14	9.00	96.47	0.585
4	5	Block 1	2.50	11.90	9.00	1.7	1.075
17	6	Block 1	1.50	7.14	9.00	99.97	0.615
5	7	Block 1	0.50	7.14	2.00	12.88	0.1518
13	8	Block 1	1.50	7.14	9.00	97.75	0.57
7	9	Block 1	0.50	7.14	16.00	84.94	1.1172
1	10	Block 1	0.50	2.38	9.00	99.42	0.14
3	11	Block 1	0.50	11.90	9.00	99.82	1.25
10	12	Block 1	1.50	11.90	2.00	44.29	0.2915
9	13	Block 1	1.50	2.38	2.00	1.89	0.033
2	14	Block 1	2.50	2.38	9.00	44.01	0.185
11	15	Block 1	1.50	2.38	16.00	64.22	0.3014
8	1	Block 1	2.50	7.14	16.00	98.42	1.064
14	17	Block 1	1.50	7.14	9.00	98.35	0.585

coded by three levels designated as  $-1$  (low),  $0$  (center),  $+1$  (high) as shown in Table S1. All the statistical plots have been generated by the software Design-Expert V-6.0.8. The experimental range for each process parameter was determined based on a literature survey and preliminary tests [10,40]. In this study, there were 17 experimental runs designed by BBD under a three-level factorial design, as shown in Table 1. The efficacy of the EO process was determined by analyzing the responses of % inactivation ( $Q_1$ ) and energy consumption ( $Q_2$ ). The energy consumption ( $E$ ) in (kWhrm<sup>-3</sup>) and % inactivation was calculated by the Equation (1) [41].

$$E = V \times I \times t / S_v \quad \& \quad \begin{aligned} \% \text{ Inactivation} &= (\text{Initial conc.} - \text{Final conc.}) / \\ &\text{Initial conc.} \times 100. \end{aligned} \quad (1)$$

Here,  $V$  = voltage,  $I$  = current (A),  $t$  = treatment time (h) and  $S_v$  = volume of sample in (m<sup>3</sup>).

To fit the experimental data of the input variables on the response  $Q$ , a second-order polynomial equation (2) was used by considering all square terms, linear terms, and linear by linear interaction terms, the quadratic response model [42] can be expressed as:

$$Z = a_0 + \sum_{i=1}^4 \alpha_i X_i + \sum_{i=1}^4 \alpha_i X_i^2 + \sum_{i=j}^3 \sum_{i=j+1}^4 \alpha_{ij} X_{ij} + ei. \quad (2)$$

Here,  $Z$  is the response,  $\alpha_o$ ,  $\alpha$ ,  $\alpha_{ii}$ , and  $\alpha_{ij}$  are the constant coefficients,  $X_i$ ,  $X_{ii}$ , and  $X_{ij}$  are the input variables, and  $ei$  is the error. The  $F$ -test, lack of fit test, and other measures were used for the acceptability of the chosen polynomial model. In this study, two responses are involved, i.e. (% inactivation and energy consumption). Therefore, the multiple response process optimization and the desirability function approach were used to optimize the input parameters of the EO process [43,44]. The value of the desirability function lies between 0 and 1, indicating the prudence of the response to its ideal value [45].

### 3. Results and discussion

#### 3.1. Statistical analysis with BBD

The BBD of RSM developed by a statistical Design-Expert software of 6.0.8 version (STAT-Ease Inc., Minneapolis, US) was used for the EO bacteria treatment.

The results of % inactivation and energy consumption were analysed by the EO experimental runs suggested by the BBD design set process, as shown in Table 1. The lack of fit tests, sequential model sum of squares, and model summary statistics tests were used to select the best regression models among various other models of linear, modified, mean, cubic, 2FI, and quadratic [46,47]. Among the nine transformations of RSM, the none transformation was used for both the responses, and the cubic and quadratic models were used to analyse % inactivation and energy consumption, respectively. The model summary statistics for % inactivation showed the cubic model's  $R^2$  and adjusted  $R^2$  values to be 0.997 and 0.9987, respectively. The cubic model here is aliased. In the case of the quadratic model, the  $R^2$  and adjusted  $R$  values for energy consumption were 0.9987 and 0.9971, respectively. Here, the quadratic model is suggested.

The relationship between the responses and the input parameters in terms of coded factors obtained from the RSM software were expressed by the quadratic model equation as shown in Equations (3) and (4).

$$\begin{aligned} \% \text{ Inactivation} = & +97.85 + 4.60 \times X_1 + 19.45 \times X_2 \\ & + 29.41 \times X_3 - 17.80 \times X_1^2 - 18.81X_2^2 - 26.54 \times X_3^2 \\ & - 10.68 \times X_1 \times X_2 + 2.14 \times X_1 \times X_3 \\ & - 1.75 \times X_2 \times X_3 - 29.92 \times X_1^2 X_2 + 8.76 \times X_1^2 \times X_3 \\ & - 42.98 \times X_1 \times X_1^2 \end{aligned} \quad (3)$$

$$\begin{aligned} \text{Energy consumption} = & +0.58 - 0.026 \times X_1 \\ & + 0.49 \times X_2 + 0.48 \times X_3 + 0.023 \times X_1^2 \\ & + 0.064 \times X_2^2 + 0.016 \times X_3^2 - 0.055 \times X_1 \times X_2 \\ & - 6.700 \times 10^{-3} \times X_1 \times X_3 + 0.36 \times X_2 \times X_3 \end{aligned} \quad (4)$$

where  $X_1$ ,  $X_2$ ,  $X_3$ , are NaCl dose, current density and treatment time respectively.

The analysis of variance (ANOVA) results is shown in Table 2, obtained from the second-order polynomial equation for both the responses for the EO treatment of bacteria using MMO. The model  $F$ -values 1011.24 and 619.97 for % inactivation and energy consumption, respectively, imply that the model is significant. Values of "Prob >  $F$ " < 0.05 indicate that the model terms are significant [48]. There is only a 0.01% chance that the "Model- $F$  values" this large could occur due to the noise. In case of % inactivation, the ANOVA results suggests that the model terms, NaCl dose, current density, time, NaCl dose<sup>2</sup>,

current density<sup>2</sup>, time<sup>2</sup>, NaCl dose  $\times$  current density, NaCl dose  $\times$  time, NaCl dose<sup>2</sup> current density, NaCl dose<sup>2</sup> time, NaCl dose current density<sup>2</sup> are significant terms. For energy consumption, the significant model terms are NaCl dose, current density, time, current density<sup>2</sup>, NaCl dose  $\times$  current density, and current density  $\times$  time. The adequate precision ratio was 79.548 and 91.025 for % inactivation and energy consumption, respectively. A ratio greater than 4 indicates that the model is desirable and can be used to navigate the design space [49].

The diagnostic plots for the actual versus predicted experimental values were analysed to evaluate the data points and check the mathematical model's accuracy. These plots indicate the relation between the predicted and the actual experimental values [50]. The data points for this plot are very close to the straight diagonal line, thus suggesting a good relationship between the actual experimental values and the predicted data values by the mathematical model, as shown in Figure S1 [51]. To study the effect of the operational parameters on both the responses, the 3D response surface graphs were analysed for each parameter.

### 3.2. Effect of process parameters

#### 3.2.1. Effect of current density ( $j$ ) on % inactivation

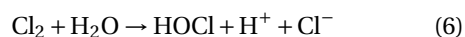
Current density is one of the significant process parameters in the EO treatment from both cost-effectiveness and mechanistic study point of view. The generation of ROS and RCS on the electrodes [52] and the electron transfer mechanism depend on the current density values by following reactions (5)–(11) [30]. The maximum inactivation efficiency at acidic pH was due to the adsorption rate of  $\bullet\text{OH}$  on the surface of MMO anode was high which leads to direct oxidation of contaminants, as at basic pH, the adsorption rate of  $\bullet\text{OH}$  decreases due to transformation of  $\bullet\text{OH}$  into lower potential oxidants like  $\text{H}_2\text{O}_2$  and  $\text{HO}_2\bullet$ . Moreover, at acidic pH, the production rate of high potential oxidants like  $\text{HOCl}$ ,  $\text{Cl}_2$ ,  $\text{ClO}^-$  was maximum. Furthermore, the pH of the solution during the EO process was  $\sim 4.5$  [53]. The production rate of chloro-oxidant species increases by increasing the  $j$  value up to a certain limit which also depends on the  $n$  value [54]. The EO treatment process works best at low  $j$  values with MMO because

**Table 2.** The table shows the ANOVA results as suggested by BBD for % inactivation and energy consumption

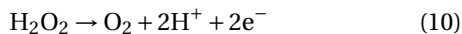
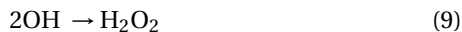
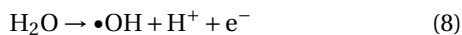
Sources	% Inactivation, ( $Q_1$ )					Energy consumption, ( $Q_2$ )				
	Sum of square	DF	Mean square	F-value	Prob > F	Sum of square	DF	Mean square	F-value	Prob > F
Model	24,143.53	12	2011.96	1011.24	<0.0001	4.38	9	0.49	619.97	<0.0001
$X_1$	84.55	1	84.55	42.49	0.0029	$5.492 \times 10^{-3}$	1	$5.492 \times 10^{-3}$	6.99	0.0333
$X_2$	1512.82	1	1512.82	760.36	<0.0001	1.95	1	1.95	2484.57	<0.0001
$X_3$	3460.38	1	3460.38	1739.23	<0.0001	1.88	1	1.88	2389.69	<0.0001
$X_1^2$	1334.63	1	1334.63	670.80	<0.0001	$2.215 \times 10^{-3}$	1	$2.215 \times 10^{-3}$	2.82	0.1370
$X_2^2$	1489.55	1	1489.55	748.67	<0.0001	0.017	1	0.017	21.65	0.0023
$X_3^2$	2965.50	1	2965.50	149.50	<0.0001	$1.033 \times 10^{-3}$	1	$1.033 \times 10^{-3}$	1.31	0.2893
$X_1 X_2$	456.04	1	456.04	229.21	0.0001	0.012	1	0.012	15.40	0.0057
$X_1 X_3$	18.36	1	18.36	9.23	0.0385	$1.796 \times 10^{-4}$	1	$1.796 \times 10^{-4}$	0.23	0.6472
$X_2 X_3$	12.29	1	12.29	6.17	0.0679	0.51	1	0.51	655.23	<0.0001
$X_1 X_3$	333.06	1	333.06	69.92	<0.0001					
$X_1^3$	0.000	0								
$X_2^3$	0.000	0								
$X_3^3$	0.000	0								
$X_1^2 X_2$	1791.01	1	1791.01	900.19	<0.0001					
$X_1^2 X_3$	153.48	1	153.48	77.14	0.0009					
$X_1 X_2^2$	3694.56	1	3694.56	1856.94	<0.0001					
$X_1 X_3^2$	0.000	0								
$X_2^2 X_3$	0.000	0								
$X_2 X_3^2$	0.000	0								
$X_1 X_2 X_3$	0.000	0								
Pure error	7.96	4	1.99			$4.320 \times 10^{-3}$	4	$1.080 \times 10^{-3}$		
Cor total	24,151.49	16				4.39	16			
Residual	—					$5.501 \times 10^{-3}$	7	$7.858 \times 10^{-4}$		
Lack of fit	—					$1.181 \times 10^{-3}$	3	$3.935 \times 10^{-4}$	0.36	0.7834

of the low oxygen evolution potential, as there is no side reaction and therefore increases the process efficiency. From Figure 2a, the effect of  $j$  and  $n$  on % inactivation can be analyzed. With the increase in  $j$  values from 2.38 to 11.90 mA/cm<sup>2</sup>, there is a gradual decrease in the % inactivation of bacteria. High  $j$  values would not effectively inactivate the bacteria at high electrolyte (NaCl) concentration because the effect of NaCl dose is very low which is again a significant parameter for RCS generation. Although higher  $j$  values may lead to an increase in temperature of the solution, even using only bacterial consortium alone without any organic load may also result in an increase in temperature, but the temperature increase in this situation is not enough to denature

the bacterial proteins or inactivate the bacterial enzyme. Hence, it may be concluded that electrolyte (NaCl) concentration plays an important role at high and low current densities [55]. At a low  $j$  value of 2.38 mA/cm<sup>2</sup> and a minimum  $n$  value of 0.5 g/L, the % inactivation is maximum at around 96% because of low oxygen evolution potential which disfavours other side reaction and increases the inactivation rate. Further, with a gradual increase in  $n$  value from 0.5 to 1.50 g/L, the % inactivation remains constant. But from 2.0 to 2.50 g/L, there is a gradual decrease in % inactivation.

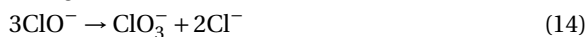
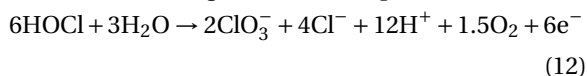






### 3.2.2. Effect of NaCl dose ( $n$ ) on % inactivation

The NaCl concentration in the EO process determines the efficiency and the amount of RCS formed during the process at MMO anodes. By increasing the  $n$ , the bacterial inactivation increases due to the formation of hypochlorite and chloride ions which get adsorbed on the surface of the anode either electrochemically or chemically as shown by the following reactions (12)–(14) [56]. At an acidic pH, the generation of HOCl oxidant species in bulk was maximum which dominates over other oxidant species like  $\text{Cl}_2$ ,  $\text{ClO}^-$ , thus leading to indirect oxidation. The production of these ions reacts with the bacterial cell leading to its inactivation either directly on the anode's surface or through  $\text{OH}\bullet$  and indirectly by RCS generated in bulk. Therefore, the maximum efficiency of this EO process is due to the synergistic effect between RCS and  $\text{OH}\bullet$  [45]. From Figure 2b, the effect of  $t$  and  $n$  on % inactivation can be analyzed. At lesser  $t$  values, the % inactivation is minimum with high  $n$ . With the gradual increase in  $t$  values, the % inactivation also increases. From 2 to 9 min, the % inactivation is minimum compared to the time values from 9 to 16 min, where a gradual increase in % inactivation can be observed. With  $n$  values of 0.5 to 1.5 g, the % inactivation increases with increasing  $t$ . Further, increase in,  $n$  values from 1.5 to 2.5 g, the % inactivation is maximum (99.59%) from 12.50 to 16 min which may be due to the synergistic effect of RCS and  $\text{OH}\bullet$  radicals which propagated maximum inactivation during the treatment process.



### 3.2.3. Effect of treatment time ( $t$ ) on % inactivation

The treatment time is a crucial operating factor in the EO process since it controls the reaction rate and affects the process economy. To analyze the effect of time and current density on % inactivation, the 3-D

graph was studied as shown in Figure 2c. At lower values of  $j$ , with an increase in  $t$ , the % inactivation was also increasing. At the same  $t$  with higher  $j$  values, the % inactivation was minimum (~35%). From  $t$  values of 12.50 to 16 min, the % inactivation was maximum (99.86%) and was constant for lower  $j$  values. According to literature, an impermeable layer is generated on the surface of the electrode during electrolysis, leading to the inactivation of the electrode surface. Hence, it increases the  $t$  of the EO process and decreases its efficiency [51]. However, no such problem was observed in this study, as the used MMO electrode links both the direct and mediated oxidation process and helps prevent electrode inactivation during electrolysis.

### 3.2.4. Effect of current density ( $j$ ) and NaCl dose ( $n$ ) on energy consumption

Energy consumption depends on the process parameters and the type of electrode used. From Figure 3a, it can be seen that with an increase in  $j$  at lower values of  $n$ , the energy consumption was maximum due to the lower solution conductivity and the increase in voltage drop. But with an increase in  $n$  at lower values of  $j$ , the energy consumption was constant. At lower  $j$  values from 2.38 to 4.76  $\text{mA}/\text{cm}^2$ , the energy consumption was maximum with an increase in  $n$ . At higher  $j$  values with increasing  $n$  values from 0.5 to 1.0  $\text{g}/\text{L}$ , the energy consumption was increasing. Further, increasing the  $n$  from 1.50 to 2.50  $\text{g}/\text{L}$  decreased the energy consumption at higher  $j$  values because of ease in flow of current through the electrolytic solution.

### 3.2.5. Effect of current density ( $j$ ) and treatment time ( $t$ ) on energy consumption

Figure 3b shows that at higher  $j$  values, the energy consumption gradually increases with  $t$  values. Such behaviour may be attributed to a decrease in ionic concentration, leading to lower conductance and other side reaction resulting in maximum energy consumption. At a low  $j$  value of 2.38  $\text{mA}/\text{cm}^2$ , the energy consumption increases with an increase in  $t$ . This might occur as the electricity consumption is directly proportional to  $t$  [43].

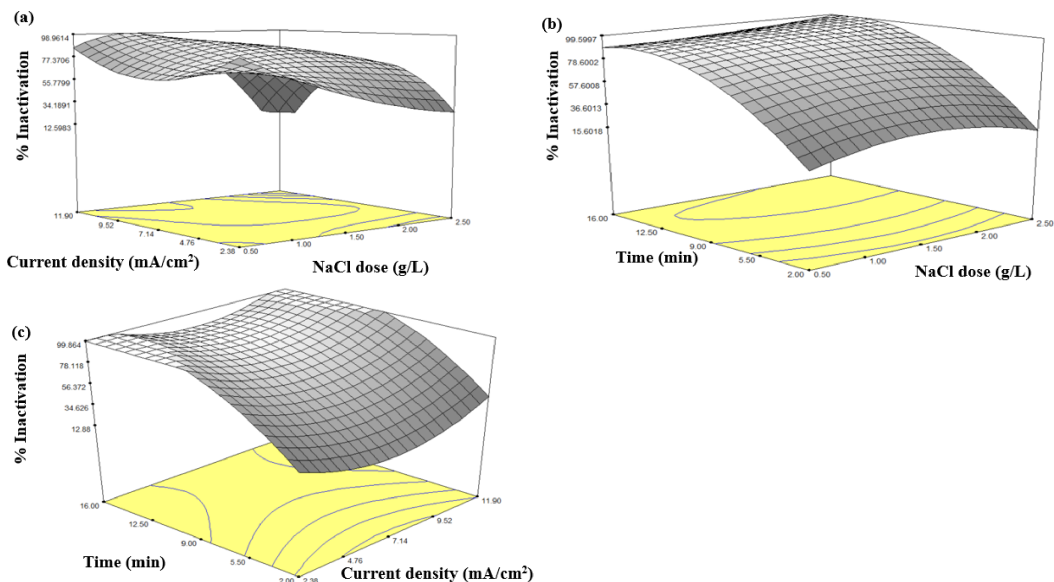


**Figure 2.** The 3D response surface graph shows the effect of process parameters on % Inactivation (a)  $j$  and  $n$ ; (b)  $t$  and  $n$ ; (c)  $t$  and  $j$ .

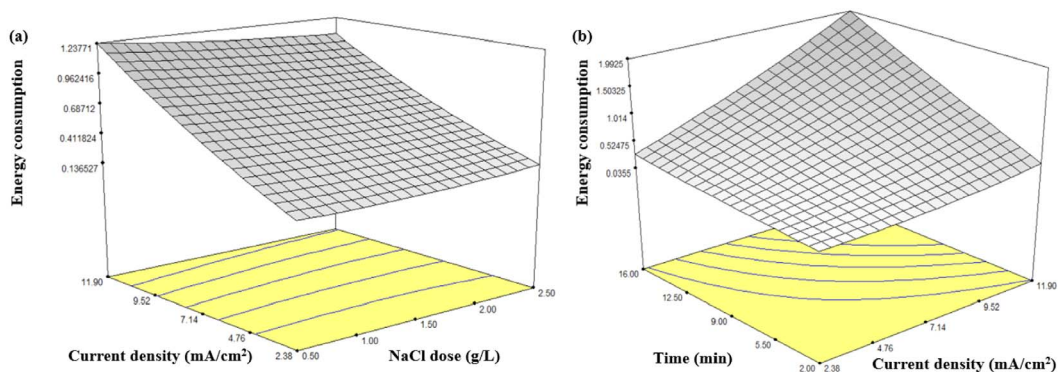


**Figure 3.** The 3D response graph showing the effect of process parameters on energy consumption (a)  $j$  and  $n$ ; (b)  $t$  and  $j$ .

### 3.3. Optimization

This study optimized the process parameters such as current density, time, and NaCl dose to get the maximum bacterial inactivation and minimum energy consumption by using MMO anodes. The optimum conditions for the two responses,  $Q_1$  and  $Q_2$ , were not the same. Using the desirability function approach, the optimum conditions for  $Q_1$  were selected as maximum, and for  $Q_2$  as a minimum. Some constraints were applied to input process parameters

to obtain this integer, as shown in Table S2.

The optimized values of the process parameters and the responses and the desirability values for individual and simultaneous optimization are shown in Table S3. The optimum conditions for the process variables were NaCl dose = 1.77 g/L, current density = 6.34 mA/cm<sup>2</sup>, time = 10 min. At this optimized condition, the responses  $Q_1$  and  $Q_2$ , as proposed by BBD, were 99.96% and 0.58 kWh/m<sup>3</sup>, respectively, along with a desirability value of  $D = 0.884$ . The experiment was performed under these optimized con-

**Table 3.** Comparative study with previous literature

Wastewater	Microbe	Technique used	Removal efficiency	Current density	References
Synthetic water	<i>Pseudomonas aeurigonosa</i>	Electrooxidation with boron doped diamond (BDD) and RuO <sub>2</sub> /IrO <sub>2</sub> DSA	>5 log-unit reduction at 30 min	33.33 mA/cm <sup>2</sup>	[57]
Synthetic urine	<i>Escherichia coli</i> , <i>Pseudomonas aeurigonosa</i>	Electrooxidation with boron doped diamond (BDD)	10 <sup>6</sup> CFU/mL removal at 60 min for <i>E. coli</i> and 120 min for <i>P. aeurigonosa</i>	5–100 A/m <sup>2</sup>	[20]
Simulated wastewater	<i>Escherichia coli</i>	Electrooxidation with graphite electrodes	3.2 log reduction at 5 min	2–8 mA/cm <sup>2</sup>	[58]
Synthetic urine	<i>Klebsiella pneumoniae</i>	Electrooxidation with mixed metal oxide (MMO)	7 log reduction before 120 min	5–50 A/m <sup>2</sup>	[59]
Synthetic urine	<i>Escherichia coli</i>	Electrooxidation with BDD, IrO <sub>2</sub> , RuO <sub>2</sub> , Pt	Complete deactivation	1.34 Ah/dm <sup>3</sup>	[9]
Simulated wastewater	<i>Escherichia coli</i> , <i>Bacillus subtilis</i> , <i>Staphylococcus aureus</i> , <i>Salmonella enterica</i> , <i>Acinetobacter calcoacetius</i> , <i>Serratia marcescens</i> , <i>Listeria</i> sp., <i>Enterococcus faecalis</i>	Electrooxidation with mixed metal oxide (MMO)	99.96% inactivation at 10 min	6.34 mA/cm <sup>2</sup>	Present study

ditions to check the developed model's efficacy. The responses,  $Q_1$  and  $Q_2$  at these optimized conditions, came out to be 99.2% and 0.42 kWh/m<sup>3</sup>, respectively. These values are very close to the ones predicted by the model, as shown in Table S4. During electrolysis, various ions like OH•, HOCl, Cl<sub>2</sub>, and Cl<sup>−</sup> were generated, leading to direct and indirect oxidation.

Further, the OH• generated in the process helps in direct oxidation and readily gets converted to H<sub>2</sub>O<sub>2</sub> and HO<sub>2</sub>•, thus leading to indirect oxidation. Further, the presence of RCS also helps in indirect oxidation. Hence, bacterial inactivation occurs due to direct and indirect oxidation at optimized conditions. Moreover, the obtained results have been critically analyzed with the reported studies as depicted in Table 3. The present study uses the novel compo-

sition of MMO anode (TiO<sub>2</sub>/IrO<sub>2</sub>/RuO<sub>2</sub>/PtO<sub>2</sub>) with low current density of 6.34 mA/cm<sup>2</sup> for the complete inactivation of bacterial consortium within a treatment time of 10 min. Thus, it is concluded that the technique is economically feasible at lower current density and treatment time.

### 3.4. Characterization of MMO anodes

#### 3.4.1. SEM/EDS analysis

To characterize the surface morphology and elemental composition of MMO anodes, SEM-EDS was performed for both fresh and recycled anodes Figure 4a,b. The SEM images for both fresh and recycled anodes show almost similar structural characteristics even after 50 cycles, thus indicating the uniform

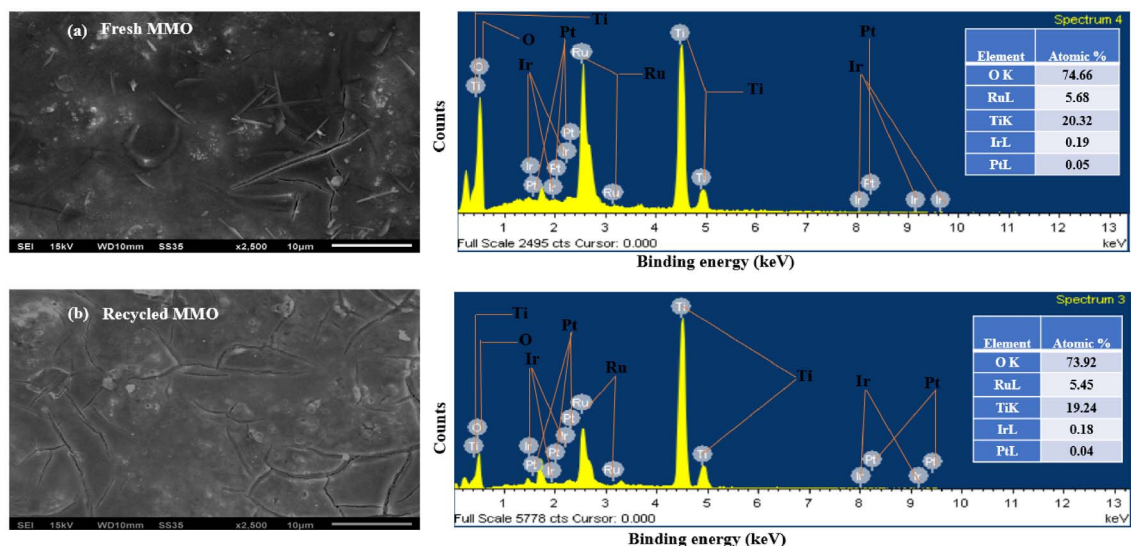


**Figure 4.** SEM and EDS images of MMO anode showing peaks of Ti, Ru, O, Ir, Pt along with their atomic composition (a) Fresh MMO and (b) Recycled MMO.

layer of metal oxides. The incorporation of Ir, Ru, and Pt oxides in the titanium metal sheet has made the electrode surface porous and smooth with slight cracks, thus preventing the electrodes from corrosion and increasing the stability for a more extended period [60]. The pronounced peaks of all the three metals, i.e., Ir, Ru, and Pt in the recycled anode, along with the peaks of Ti, and O, have proved the durability of electrodes even after 50 cycles. The quantitative analysis of the electrodes was performed by EDS. It depicts that the atomic concentration of the metal oxides of Ti, Ru, Ir, Pt, and O were almost similar for both fresh and recycled anodes after 50 cycles. Such results confirm the stability of electrodes after 50 experimental runs as shown in Figure 4a,b.

### 3.4.2. XPS analysis

The XPS spectra of both fresh and recycled anodes Figure 5 was performed in order to analyze the metal elements' oxidation state and to study the molecular information associated with electrode surface chemistry [61,62]. The results indicate no drastic change in the oxidation state of the metals as well as each metal element present after 50 cycles. As shown in Figure 5a, in the Ti 2p spectrum, the two peaks at 458.5 eV and 464.3 eV correspond to the binding en-

ergies of Ti 2p<sub>3/2</sub> and Ti 2p<sub>1/2</sub> states for both the fresh and recycled anodes [63]. Figure 5e, shows the spectrum of O 1s signal at 531.47 eV, which corresponds to a broad peak due to the formation of Ti–O bonds. Figure 5b,c and d, shows the spectrum signal of Ir 4f, Ru 3d, and Pt 4f for both fresh and recycled anodes. Pt signal spectrum is indicated at 74.2 eV. It shows the signal of the Pt (v) oxidation state at the 4f<sub>5/2</sub> level, which further corresponds to the formation of Pt–Ti bonds. However, for Ru, the peak was observed at 284.8 eV while for Ir, the peaks were observed at 61.6 eV and 63.2 eV. The signals obtained from the Ru and Ir spectrum were linked with Ru 3d<sub>3/2</sub>, and Ir 4f<sub>7/2</sub>, Ir 4f<sub>5/2</sub>, respectively, indicating the formation of hydrated metal oxides of RuO<sub>2</sub> and IrO<sub>2</sub>. The studies reported in the previous literature correspond to the results in the present study [64–66].

### 3.4.3. XRD analysis

The X-ray diffraction study was performed for both fresh and recycled MMO anodes. The XRD analysis was applied to study the crystalline structure of the metal oxides coated on titanium sheet. Further, prominent peaks of the metal oxides of Ti, Ru, Ir and, Pt was observed in the recycled anode even after 50 experimental runs thus proving the metals' intactness as shown in Figure S2. The diffraction peaks

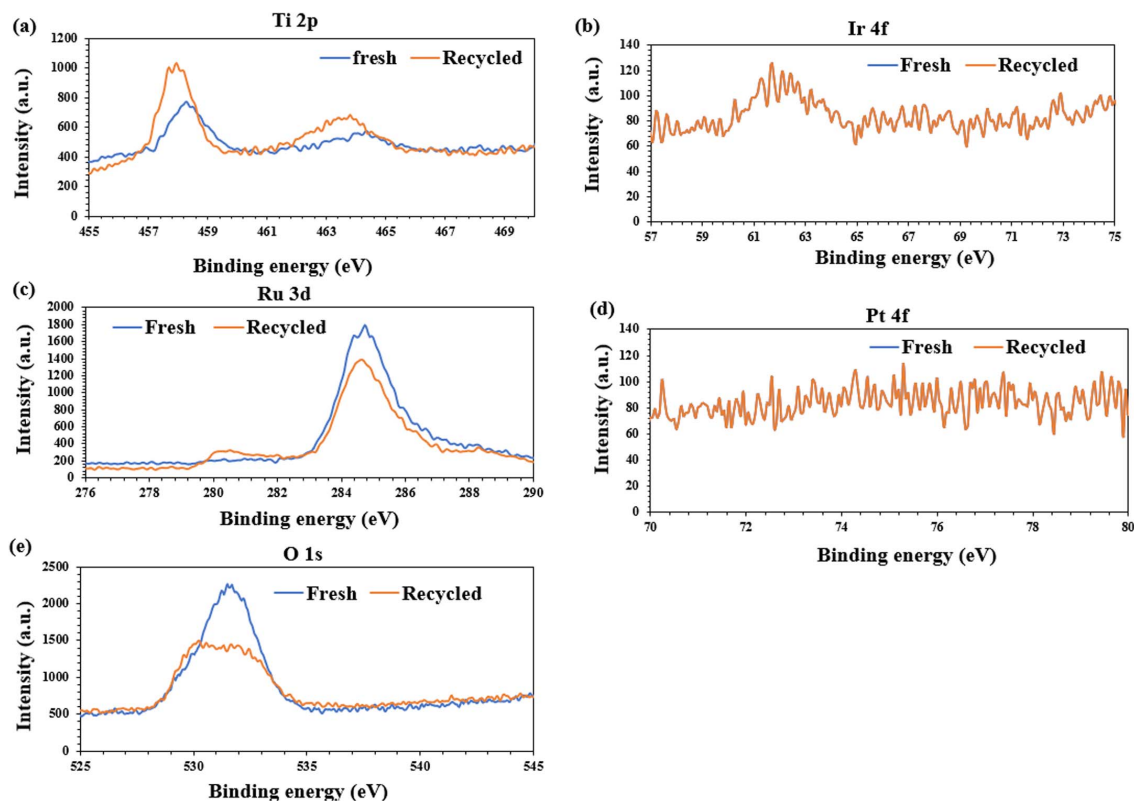


**Figure 5.** XPS graph of both fresh and recycled MMO long with their spectrum (a) Ti 2p, (b) Ir 4f, (c) Ru 3d, (d) Pt 4f and (e) O 1s.

of titanium (JCPDS card: 01-089-3073), titanium oxide (JCPDS card: 01-089-8303), iridium oxide (JCPDS card: 01-088-0288), ruthenium oxide (JCPDS card: 00-040-1290), and platinum oxide (JCPDS card: 00-021-0613).

#### 3.4.4. Electrochemical analysis

The cyclic voltammetry (CV) study was done in order to characterize the electrochemical activity of MMO anodes as shown in Figure S3. The reference electrode was a calomel electrode with platinum as a counter electrode with a scanning rate of 500 mV/s. The full CV scan of the MMO anode was recorded in the potential range of  $-1.0$  to  $0.4$  V. As it can be seen that for cycle 1 the oxidation peak was observed at  $\sim 7$  mA, but for cycles 15, 30, 45 and, 50 the oxidation peak was stable at  $\sim 20$  mA. Thus, the stability of MMO anodes after 50 experimental runs is proved [67–69].

#### 3.4.5. Hydroxyl radical test

In order to see the efficacy of the EO process, EO has been performed under optimized conditions to confirm the production of  $\text{OH}\cdot$  at MMO. Experiments were performed in absence and in presence of NaCl in an aqueous solution containing 0.5 mM TPA in 1M NaOH. Figure S4s confirmed that the production of  $\text{OH}\cdot$  was maximum at 2 min, and with increasing time, the generation of  $\text{OH}\cdot$  decreased when NaCl was added to the solution. However, from Figure S4, it was concluded that the generation of  $\text{OH}\cdot$  at an acidic pH of 3.8 was maximum for 10 min. With increasing time, the generation of  $\text{OH}\cdot$  was increased when no NaCl was added to the solution. This concludes that at an acidic pH, the rate of  $\text{OH}\cdot$  adsorption is high on MMO anodes leading to the direct oxidation of the compound. To verify the synergistic effect of RCS and  $\text{OH}\cdot$ , an experiment was performed to measure the % inactivation

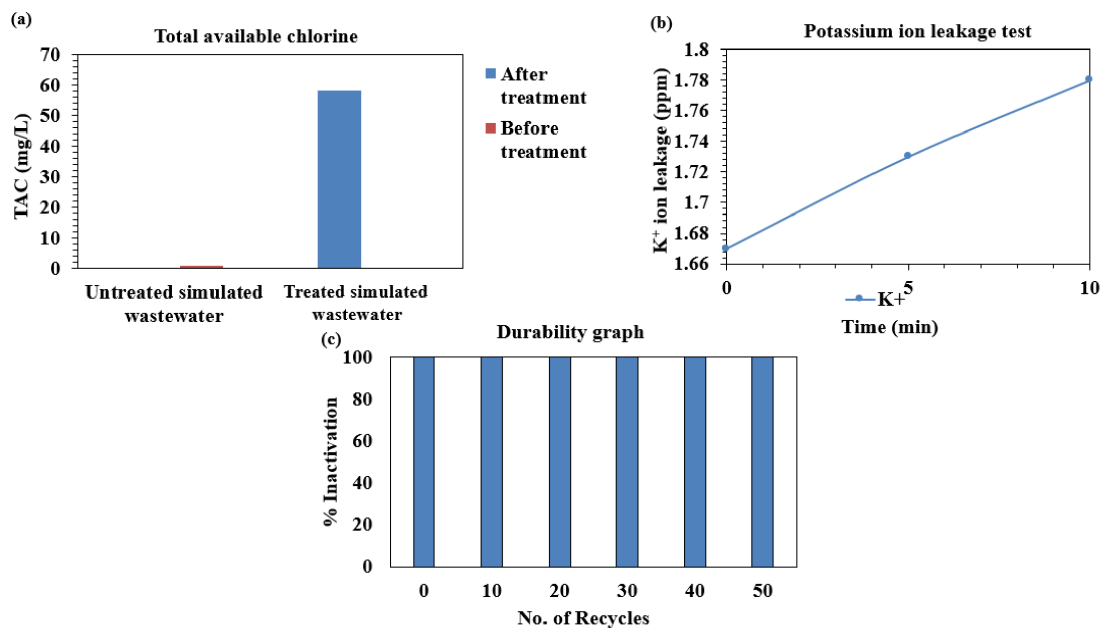


**Figure 6.** Plot of mineralization at an optimized condition of (current density =  $6.34 \text{ mA/cm}^2$ , NaCl dose =  $1.77 \text{ g}$ , time =  $10 \text{ min}$ ). (a) TAC graph of before and after treatment of simulated wastewater containing bacterial consortium. (b) Potassium ion leakage graph of simulated wastewater at different time intervals under optimized condition. (c) Durability graph of MMO anodes after 50 recycles showing no loss in the inactivation efficiency of electrodes.

rate Figure S5. Here, the absorbance of the sample solution having bacterial consortium with NaCl and TPA (scavenger of  $\text{OH}\cdot$ ) was measured at  $600 \text{ nm}$  in order to observe the effect on the % inactivation rate. No significant elimination of bacterial consortium was observed when the sample solution was treated with only current and TPA. In contrast,  $\sim 95\%$  and  $\sim 98\%$  inactivation was observed when the bacterial consortium was treated with NaCl and both NaCl and TPA respectively. Thus, it is concluded that the inactivation rate depends mainly on the RCS generation.

### 3.5. Durability study

The durability and the stability of MMO anodes have been studied in order to check the economic cost and the practical feasibility of the EO process on a commercial scale. In particular, the durability of the electrodes has been evaluated in terms of the number of recycles and the inactivation efficiency of bacteria, as shown in Figure 6c. The electrodes were thoroughly

used for 50 cycles without any significant loss of the metal oxides. Conditions for 50 cycles were according to the experimental runs as suggested in Table 1. The high activeness of the MMO anodes was due to the minimum amount of NaCl concentration used at lower current density values. Due to the presence of  $\text{IrO}_2$  in the MMO anodes, it can be used for a maximum of 5 years. These MMO anodes can produce a magnificent amount of RCS and ROS due to  $\text{TiO}_2$ ,  $\text{IrO}_2$ , and Pt, leading to direct and indirect oxidation [70]. The durability of MMO after 50 cycles was further confirmed through SEM-EDS, and XPS analysis, as discussed in Section 3.4.

### 3.6. TAC analysis (total available chlorine)

To check the quality of the untreated and treated simulated wastewater, analytical test such as TAC was performed under optimized conditions. From Figure 6a, it was observed that the TAC level increased during the EO treatment of simulated wastewater after a treatment time of  $10 \text{ min}$ . The TAC is a mixture

of reactive intermediates comprising chloramines such as ( $\text{NH}_2\text{Cl}$ ) and free chlorine ( $\text{Cl}_2$ ,  $\text{HOCl}$ ) [71]. Thus, it is concluded that the RCS produced during electrolysis using MMO anode is responsible for the inactivation of bacteria present in the simulated wastewater.

### 3.7. Bacterial cell damage checked by potassium ion leakage test

The outer membrane of the bacterial cell serves an essential function of barrier to the permeability of the intracellular substances. The bacterial cell damage was due to RCS, which damages the cell wall and the outer membrane of bacteria produced during the EO treatment of simulated wastewater. Thus, It leads to nd increased permeability and leakage of intracellular substances like  $\text{K}^+$  from the cell [11]. The leakage of  $\text{K}^+$  ions from the damaged bacterial cell was studied for 10 min. The  $\text{K}^+$  ion concentration increased from 1.63 ppm to 1.78 ppm Figure 6b. The  $\text{K}^+$  ion was released entirely from the inactivated bacterial cell after a treatment of 10 min. Thus, it is concluded that the membrane permeability of bacterial cells was disrupted during the EO process.

### 3.8. Operating cost analysis

To commercialize the EO treatment technology at large scale, it is mandatory to estimate the total cost of the treatment process, which should be economically feasible. Hence, the electrical energy consumed and the cost of the electrodes have been considered for the economic evaluation of the treatment process. The total operating cost for the inactivation of bacteria in simulated wastewater was determined to be 0.189  $\$/\text{m}^3$  (Table S5). Such value indicates that the EO process by MMO is economically feasible. Few researchers have reported the operating cost analysis for the treatment of different wastewaters [71–74]. Further, the operating cost can be minimized during the scale-up studies by modifying the design of the electrolytic reactor and the operating conditions.

## 4. Conclusion

The EO treatment of bacteria using titanium-based MMO was performed. The optimized process parameters from BBD were found to be  $\text{NaCl}$

dose = 1.77 g/L, current density =  $6.34 \text{ mA}/\text{cm}^2$ , time = 10 min for obtaining the maximum degradation. At these optimized conditions, the values of responses  $Q_1$  and  $Q_2$  were 99.2% and  $0.42 \text{ kWh}/\text{m}^3$ , respectively, and a combined desirability  $D = 0.884$ . The bacterial inactivation was found to be maximum because of both direct and indirect oxidation involvement due to the formation of strong oxidants,  $\text{OH}\cdot$  and RCS like  $\text{HOCl}$ ,  $\text{Cl}_2$ , and  $\text{Cl}^-$ . Further, TAC proved the inactivation of bacteria in simulated wastewater after a treatment time of 10 min. The characterization studies like SEM-EDS and XPS proved the stability and durability of MMO anodes for bacterial inactivation even after 50 cycles. The potassium ion leakage test further confirmed the bacterial damage. The present study indicates the efficiency of MMO anodes for further research analysis towards eco-sanitation and opens up a new approach for the on-site treatment of wastewater.

## Conflicts of interest

The authors declare no competing interest.

## Authorship statement

All authors certify that they have participated sufficiently in the work to take public responsibility for the content, including participation in the concept, design, analysis, writing, or revision of the manuscript. Furthermore, each author certifies that this material or similar material has not been and will not be submitted to or published in any other publication.

## Authorship contributions

- (1) Conception and design of the study: AV, DC, PC
- (2) Experimentation: PC
- (3) Analysis/Interpretation of Data: PC
- (4) Drafting the Manuscript: PC, AV, DC
- (5) Revising the manuscript critically for important intellectual content: AV.

## Ethics approval

Not applicable.



## Consent to participate

The authors have read and approved the final manuscript.

## Consent for publication

The authors agree to publication in this journal.

## Funding

This research did not receive any specific grant from funding agencies in the public, commercial, or not-for-profit sectors. PC is thankful to the Thapar Institute of Engineering and Technology for providing the fellowship.

## Acknowledgments

The authors would like to thank the Sophisticated Analytical Instruments Laboratories, TIET, Punjab and IIT Roorkee, India for providing their facilities for the characterization of samples.

## Supplementary data

Supporting information for this article is available on the journal's website under <https://doi.org/10.5802/crchim.225> or from the author.

## References

- [1] D. P. Mohapatra, S. K. Brar, R. D. Tyagi, P. Picard, R. Y. Surampalli, *Sci. Total Environ.*, 2014, **470**, 58-75.
- [2] Z. B. Gönder, S. Arayici, H. Barlas, *Sep. Purif. Technol.*, 2011, **76**, 292-302.
- [3] Q. Zhang, K. T. Chuang, *Adv. Environ. Res.*, 2001, **5**, 251-258.
- [4] M. Mänttari, M. Kuosa, J. Kallas, M. Nyström, *J. Membr. Sci.*, 2008, **309**, 112-119.
- [5] A. C. Rodrigues, M. Boroski, N. S. Shimada, J. C. Garcia, J. Nozaki, N. Hioka, *J. Photochem. Photobiol. A Chem.*, 2008, **194**, 1-10.
- [6] D. Ma, H. Yi, C. Lai, X. Liu, X. Huo, Z. An, L. Li, Y. Fu, B. Li, M. Zhang, *Chemosphere*, 2021, **275**, article no. 130104.
- [7] M. Herraiz-Carboné, S. Cotillas, E. Lacasa, A. Moratalla, P. Cañizares, M. A. Rodrigo, C. Sáez, *Sci. Total Environ.*, 2020, **725**, article no. 138430.
- [8] P. Chandra, A. Verma, D. Choudhury, *J. Water Process. Eng.*, 2022, **48**, article no. 102858.
- [9] S. Dbira, N. Bensalah, M. I. Ahmad, A. Bedoui, *Materials (Basel)*, 2019, **12**, article no. 1254.
- [10] J. Singla, V. K. Sangal, A. Singh, A. Verma, *J. Environ. Manage.*, 2020, **255**, article no. 109847.
- [11] I. Thakur, A. Verma, B. Örmeci, *J. Clean. Prod.*, 2022, **352**, article no. 131575.
- [12] X. Ma, N. Guo, S. Ren, S. Wang, Y. Wang, *Environ. Int.*, 2019, **126**, 127-133.
- [13] O. P. Sahu, P. K. Chaudhari, *J. Electroanal. Chem.*, 2015, **739**, 122-129.
- [14] B. Nasr, G. Abdellatif, P. Cañizares, C. Sáez, J. Lobato, M. A. Rodrigo, *Environ. Sci. Technol.*, 2005, **39**, 7234-7239.
- [15] P. Cañizares, A. Gadri, J. Lobato, B. Nasr, R. Paz, M. A. Rodrigo, C. Saez, *Ind. Eng. Chem. Res.*, 2006, **45**, 3468-3473.
- [16] P. Cañizares, B. Louhichi, A. Gadri, B. Nasr, R. Paz, M. A. Rodrigo, C. Saez, *J. Hazard. Mater.*, 2007, **146**, 552-557.
- [17] N. Rabaaoui, M. E. K. Saad, Y. Moussaoui, M. S. Allagui, A. Bedoui, E. Elaloui, *J. Hazard. Mater.*, 2013, **250**, 447-453.
- [18] N. Bensalah, A. Bedoui, *Environ. Technol.*, 2017, **38**, 2979-2987.
- [19] J. Wu, H. Zhang, N. Oturan, Y. Wang, L. Chen, M. A. Oturan, *Chemosphere*, 2012, **87**, 614-620.
- [20] S. Cotillas, E. Lacasa, C. Sáez, P. Cañizares, M. A. Rodrigo, *Appl. Catal. B Environ.*, 2018, **229**, 63-70.
- [21] A. S. Raut, G. B. Cunningham, C. B. Parker, E. J. D. Klem, B. R. Stoner, M. A. Deshusses, J. T. Glass, *ECS Trans.*, 2013, **53**, 1-11.
- [22] A. Baddouh, G. G. Bessegato, M. M. Rguiti, B. El Ibrahimi, L. Bazzi, M. Hilali, M. V. B. Zanoni, *J. Environ. Chem. Eng.*, 2018, **6**, 2041-2047.
- [23] K. Gurung, M. C. Ncibi, M. Shestakova, M. Sillanpää, *Appl. Catal. B Environ.*, 2018, **221**, 329-338.
- [24] E. Isarain-Chávez, M. D. Baró, E. Rossinyol, U. Morales-Ortiz, J. Sort, E. Brillas, E. Pellicer, *Electrochim. Acta*, 2017, **244**, 199-208.
- [25] M. R. Cruz-Díaz, E. P. Rivero, F. A. Rodríguez, R. Domínguez-Bautista, *Electrochim. Acta*, 2018, **260**, 726-737.
- [26] M. Zahedi, K. Jafarzadeh, M. Mirjani, H. M. Abbasi, *Ionics (Kiel)*, 2018, **24**, 451-458.
- [27] M. Zhou, H. Särkkä, M. Sillanpää, *Sep. Purif. Technol.*, 2011, **78**, 290-297.
- [28] H. Särkkä, K. Kuhmonen, M. Vepsäläinen, M. Pulliainen, J. Selin, P. Rantala, E. Kukkamäki, M. Sillanpää, *Environ. Technol.*, 2009, **30**, 885-892.
- [29] H. Zöllig, A. Remmele, C. Fritzsche, E. Morgenroth, K. M. Udert, *Environ. Sci. Technol.*, 2015, **49**, 11062-11069.
- [30] W. Wu, Z. H. Huang, T. T. Lim, *Appl. Catal. A Gen.*, 2014, **480**, 58-78.
- [31] J. Singla, A. Verma, V. K. Sangal, *J. Electrochem. Soc.*, 2017, **164**, E312-E320.
- [32] M. Cho, J. Kim, J. Y. Kim, J. Yoon, J.-H. Kim, *Water Res.*, 2010, **44**, 3410-3418.
- [33] J. Jeong, C. Kim, J. Yoon, *Water Res.*, 2009, **43**, 895-901.
- [34] X. Huang, Y. Qu, C. A. Cid, C. Finke, M. R. Hoffmann, K. Lim, S. C. Jiang, *Water Res.*, 2016, **92**, 164-172.
- [35] D. Ghernaout, *EC Microbiol.*, 2017, **9**, 160-169.
- [36] R. Kaur, B. Yadav, R. D. Tyagi, *Current Developments in Biotechnology and Bioengineering*, Elsevier, 2020, 103-148 pages.
- [37] J. Singla, V. K. Sangal, A. Verma, *Process. Saf. Environ. Prot.*, 2019, **130**, 197-208.



- [38] S. Bansal, J. P. Kushwaha, V. K. Sangal, *Water Environ. Res.*, 2013, **85**, 2294-2306.
- [39] P. Singh, A. Dhir, V. K. Sangal, *Desalin. Water Treat.*, 2015, **55**, 1501-1508.
- [40] R. Kaur, J. P. Kushwaha, N. Singh, *Sci. Total Environ.*, 2019, **677**, 84-97.
- [41] D. Lutic, A. M. Sescu, S. Siamer, M. Harja, L. Favier, *C. R. Chim.*, 2022, **25**, 1-13.
- [42] V. K. Sangal, V. Kumar, I. M. Mishra, *Comput. Chem. Eng.*, 2012, **40**, 33-40.
- [43] B. Mondal, V. C. Srivastava, J. P. Kushwaha, R. Bhatnagar, S. Singh, I. D. Mall, *Sep. Purif. Technol.*, 2013, **109**, 135-143.
- [44] V. K. Sangal, V. Kumar, I. M. Mishra, *Chem. Eng. Commun.*, 2014, **201**, 72-87.
- [45] A. D. Hiwarkar, S. Singh, V. C. Srivastava, I. D. Mall, *J. Environ. Manage.*, 2017, **198**, 144-152.
- [46] P. Kaur, V. K. Sangal, J. P. Kushwaha, *RSC Adv.*, 2015, **5**, 34663-34671.
- [47] K. Thirugnanasambandham, V. Sivakumar, J. P. Maran, *J. Taiwan Inst. Chem. Eng.*, 2015, **46**, 160-167.
- [48] P. Asaithambi, M. Matheswaran, *Arab. J. Chem.*, 2016, **9**, S981-S987.
- [49] V. S. Jagati, V. C. Srivastava, B. Prasad, *Sep. Sci. Technol.*, 2015, **50**, 181-190.
- [50] V. K. Sangal, V. Kumar, M. I. Mishra, *Chem. Ind. Chem. Eng. Quarterly/CICEQ.*, 2013, **19**, 107-119.
- [51] S. Singh, S. Singh, S. L. Lo, N. Kumar, *J. Taiwan Inst. Chem. Eng.*, 2016, **67**, 385-396.
- [52] H. Särkkä, A. Bhatnagar, M. Sillanpää, *J. Electroanal. Chem.*, 2015, **754**, 46-56.
- [53] H. Akrouit, L. Bousselmi, *Desalin. Water Treat.*, 2012, **46**, 171-181.
- [54] S. Dbira, N. Bensalah, A. Bedoui, *Environ. Technol.*, 2016, **37**, 2993-3001.
- [55] K. K. Garg, B. Prasad, *J. Taiwan Inst. Chem. Eng.*, 2015, **56**, 122-130.
- [56] C. Barrera-Díaz, P. Cañizares, F. J. Fernández, R. Natividad, M. A. Rodrigo, *J. Mex. Chem. Soc.*, 2014, **58**, 256-275.
- [57] C. Bruguera-Casamada, I. Sirés, E. Brillas, R. M. Araujo, *Sep. Purif. Technol.*, 2017, **178**, 224-231.
- [58] M. S. Hellal, B. A. Hemdan, M. Youssef, G. E. El-Taweel, E. M. Abou Taleb, *Sci. Rep.*, 2022, **12**, 1-12.
- [59] M. Herráiz-Carboné, E. Lacasa, S. Cotillas, M. Vasileva, P. Cañizares, M. A. Rodrigo, C. Sáez, *Chem. Eng. J.*, 2021, **409**, article no. 128253.
- [60] A. Kumar, B. Prasad, I. M. Mishra, *Chem. Eng. Technol. Ind. Chem. Equip. Process. Eng.*, 2007, **30**, 932-937.
- [61] J.-Z. Kong, A.-D. Li, X.-Y. Li, H.-F. Zhai, W.-Q. Zhang, Y.-P. Gong, H. Li, D. Wu, *J. Solid State Chem.*, 2010, **183**, 1359-1364.
- [62] A. I. Del Río, J. Fernández, J. Molina, J. Bonastre, F. Cases, *Electrochim. Acta*, 2010, **55**, 7282-7289.
- [63] W. J. Tseng, C. Cheng, J. H. Hsieh, *J. Am. Ceram. Soc.*, 2014, **97**, 407-412.
- [64] K. V. Egorov, Y. Y. Lebedinskii, A. A. Soloviev, A. A. Chouprik, A. Y. Azarov, A. M. Markeev, *Appl. Surf. Sci.*, 2017, **419**, 107-113.
- [65] N. Wang, D. Li, L. Yu, X. J. Yu, T. Y. Sun, *Int. J. Electrochem. Sci.*, 2015, **10**, 9824-9836.
- [66] L. Saravanan, C.-M. Tseng, C.-C. Chang, Y.-C. Chung, C.-Y. Lin, A.-Y. Lo, *C. R. Chim.*, 2020, **23**, 343-356.
- [67] H. Q. Pham, T. T. Huynh, H. N. Bich, T. M. Pham, S. T. Nguyen, L. T. Lu, V. T. Thanh Ho, *C. R. Chim.*, 2019, **22**, 829-837.
- [68] M. A. Kumar, V. Lakshminarayanan, S. S. Ramamurthy, *C. R. Chim.*, 2019, **22**, 58-72.
- [69] L. Kiss, S. Kunsági-Máté, *C. R. Chim.*, 2019, **22**, 557-561.
- [70] B. P. Chaplin, *Environ. Sci. Process. Impacts*, 2014, **16**, 1182-1203.
- [71] J. Singla, I. Thakur, V. Sangal, A. Verma, *Chemosphere*, 2021, **285**, article no. 131498.
- [72] R. Chauhan, V. C. Srivastava, *Chem. Eng. J.*, 2020, **386**, article no. 122065.
- [73] R. Chauhan, V. C. Srivastava, *Process Saf. Environ. Prot.*, 2021, **147**, 245-258.
- [74] S. Mahesh, K. K. Garg, V. C. Srivastava, I. M. Mishra, B. Prasad, I. D. Mall, *RSC Adv.*, 2016, **6**, 16223-16233.